Intermittent bioirrigation and oxygen dynamics in permeable sediments: An experimental and modeling study of three tellinid bivalves

Nils Volkenborn[1,7], Christof Meile[2], Lubos Polerecky[3], Conrad A. Pilditch[4], Alf Norkko[5], Joanna Norkko[5], Judi E. Hewitt[6], Simon F. Thrush[6], David S. Wethey[1] and Sarah A. Woodin[1]

[1] Department of Biological Sciences, University of South Carolina, Columbia, South Carolina 29208, USA

[2] Department of Marine Sciences, University of Georgia, Athens, Georgia 30602, USA

[3] Max Planck Institute for Marine Microbiology, 28359 Bremen, Germany

[4] Department of Biological Sciences, University of Waikato, Hamilton 3240, New Zealand

[5] Tvärminne Zoological Station, University of Helsinki, 10900 Hanko, Finland

[6] National Institute of Water and Atmospheric Research, Hamilton 2005, New Zealand

[7] corresponding author: nils@biol.sc.edu

Abstract

To explore the dynamic nature of geochemical conditions in bioirrigated marine permeable sediments, we studied the hydraulic activity of 3 tellinacean bivalve molluscs (the Pacific species *Macoma nasuta* and *Macomona liliana*, and the northern Atlantic and Pacific species *Macoma balthica*). We combined porewater pressure sensing, time–lapse photography and oxygen imaging to quantify the durations and frequencies of tellinid irrigation activity and the associated oxygen dynamics in the sediment. Porewater pressure records of all tellinids were dominated by intermittent porewater pressurization, induced by periodic water injection into the sediment through their excurrent siphons, which resulted in intermittent oxygen supply to subsurface sediments. The durations of irrigation (2–12 min long) and intervals between subsequent irrigation bouts (1.5–13 min) varied among tellinid species and individual sizes. For large *M. liliana* and *M. nasuta*, the average durations of intervals between irrigation bouts were sufficiently long (10 min and 4 min, respectively) to allow complete oxygen consumption in between irrigation bouts in all tested sediment types. Irrigation patterns of smaller conspecifics and the smaller species *M. balthica* were characterized by significantly shorter separation of irrigation bouts, which resulted in more continuous oxygenation of the sediment. Transport-reaction modeling confirmed these species– and size–specific geochemical signatures and indicated that the geochemical character of the sediment is largely conditioned by the interplay between temporal irrigation patterns and sedimentary oxygen consumption rates. For large tellinids, model simulations indicated that oscillatory rather than stationary geochemical conditions are prevalent in a wide range of sediment types, with oxic pockets collapsing completely between periods of active irrigation. Based on the model results we developed analytical approximations that allow estimation of spatio-temporal characteristics of sediment

oxygenation for a wide range of sediment types and infaunal activity patterns. Our results emphasize the need to consider the intermittent nature of bioirrigation when studying the geochemical impact of infauna in permeable sediments.

1. Introduction

Bioturbation by infaunal organisms has diverse impacts on the functioning and ecology of benthic systems. It alters the sediment characteristics and the distribution of porewater constituents (Aller, 1980; Boudreau and Marinelli, 1994; Berg *et al.*, 2001; Volkenborn *et al.*, 2007), affects microbial diversity and rates of microbially mediated processes (Aller and Yingst, 1985; Kristensen, 1988; Na *et al.*, 2008), and influences the structure of micro–, meio– and macrofaunal benthic communities (Reise, 1981; Meyers *et al.*, 1987; Woodin *et al.,* 1998; Marinelli *et al.*, 2002; Volkenborn and Reise, 2006; Engel *et al.*, 2012). The significant impact of single or multiple species on benthic–pelagic exchange fluxes is well documented (Vopel *et al.*, 2003; Lohrer *et al.*, 2004; Karlson *et al.*, 2007; D'Andrea and DeWitt, 2009, Michaud *et al.*, 2009), but time–integrated approaches such as benthic chamber incubations are likely to average over the dynamic nature of sediment reworking (Solan *et al.*, 2004) and porewater bio-advection (Wethey *et al.,* 2008; Volkenborn *et al.*, 2010). Bioturbation is the product of infaunal activities, e.g. burrowing, pumping, feeding, or defecating, and consequently the rates and direction of particle movement and fluid flow depend on the frequencies, durations, and the sequence of behaviors. A number of experimental studies have shown that infaunal organisms irrigate their burrows in a discontinuous fashion on a timescale of minutes (e.g. Kristensen *et al.*, 1991) to hours (e.g., in intertidal areas where the ventilation by infaunal organisms ceases during ebb tide; Aller and Yingst, 1978; Aller *et al.*, 1983), implying that bioturbated sediments are subject to

dynamic geochemical conditions on this time scale (Timmermann *et al.*, 2006; Volkenborn *et al.*, 2010, 2012). Typically, irrigation activity patterns are governed by endogenous pacemakers, but for many organisms they are also altered in response to changes in environmental conditions (e.g., O_2 concentration in the irrigated water; Dales *et al.*, 1970).

For a better mechanistic understanding of how infaunal organisms affect biogeochemical processes, it is essential to perform measurements and modeling on temporal and spatial scales that reflect the activities of individual organisms. The need to implement discontinuous irrigation into bioirrigation models was first addressed by Boudreau and Marinelli (1994), who developed a derivative of the cylinder microenvironment model introduced by Aller (1980) to estimate the time dependence of solute fluxes. In diffusion–dominated systems intermittent flushing of burrows causes strong temporal variations in the instantaneous solute fluxes (Boudreau and Marinelli, 1994). In advection–dominated systems the role of intermittent irrigation is less well understood, though larger sediment volumes are supplied with reactive chemical species. The pocket injection model developed by Meysman *et al.* (2005) captures the main spatial features of porewater advection when water is forced into and through permeable sediments continuously and at a constant rate, but its implementation under intermittent irrigation conditions is lacking. As recently shown for some important bioirrigating organisms such as arenicolid polychaetes and thalassinid crustaceans, bioadvective porewater transport is driven by species– and behavior–specific porewater pressure dynamics (Wethey *et al.*, 2008; Woodin *et al.*, 2010; Volkenborn *et al.*, 2010, 2012). These pressure gradients can be detected tens of centimeters away from the organisms and result in unsteady and bidirectional porewater transport (Wethey and Woodin, 2005; Wethey *et al.*, 2008; Volkenborn *et al.*, 2010). As a consequence, substantial sediment

volumes surrounding infaunal organisms and their burrows experience intermittent oxygen supply and frequent oscillations between oxic and anoxic conditions (Volkenborn *et al.*, 2012).

This study provides experimental evidence that links hydraulic activities of bioirrigating infauna with oscillation of geochemical conditions in sediments, using three tellinid bivalve mollusc species as model organisms. Tellinids are cosmopolitan nearshore bivalves with separate inhalant and excurrent siphons. They are facultative deposit- and suspension feeders (Levinton, 1991). While the inhalant siphon is used for the uptake of surface particles and overlying water, the excurrent siphon remains several cm deep in the sediment. During feeding, water passes through the bivalves and is injected into the sediment at a depth of 2–10 cm, resulting in intermittent sediment pressurization (Woodin *et al.*, 2010, 2012). Here we have investigated temporal patterns of bioirrigation associated with deposit-feeding by tellinid bivalves and their impact on oxygen dynamics in different sediment types.

Our focus is on the dynamics of O_2 as the energetically most favorable electron acceptor in biogeochemical reactions and as a widely used proxy for organic matter mineralization (see review by Glud, 2008). Specifically, we explore the volume of sediment that is characterized by either permanently oxic or intermittently oxic conditions, which can be regarded as geochemically distinct environments (Aller, 1994). Sediments experimentally exposed to oxic–anoxic oscillatory conditions – at least on the scale of days to weeks (we are not aware of studies at minute to hour timescales) – have been shown to exhibit higher mineralization rates of organic matter, including pollutants, than those with stable redox conditions (Sun *et al.*, 1993; Aller, 1994; Sun *et al.*, 2002; Caradec *et al.*, 2004; Cravo-Laureau *et al.*, 2011; Bennett *et al.*, 2012).

Given these changes in mineralization rates, quantification of the frequencies of redox oscillation and time scales of the behaviors driving these rates is critical. Focusing on redox oscillations and using empirical data, we parameterized a transport-reaction model to estimate the relationship between temporal irrigation patterns and (intermittently) oxic sediment volumes in a wide range of sediment types inhabited by these bivalves and by other important bioturbating organisms.

2. Methods

Hydraulic activities of tellinid species were investigated in laboratory containers and narrow aquaria using isolated individuals. Porewater pressure sensing was combined with time–lapse photography to identify porewater pressure waveforms associated with specific tellinid behaviors (as previously described in Volkenborn *et al.*, 2010; for pressure sensor specifications see Wethey and Woodin, 2005; Volkenborn *et al.*, 2012). Time synchronized planar optode imaging of oxygen was used to investigate the related oxygen dynamics in the porewater (for details see Matsui *et al.*, 2011; Volkenborn *et al.*, 2012). The experimental set–up differed among species, and the detailed information on aquarium sizes, overlying water exchange rates, sediment characteristics, temperature, light, salinity and experimental replication and duration are given below. In all experiments, sediments were sieved through a coarse mesh (5–10 mm) to remove larger organisms. In parallel to the aquaria setup, sediment cores (10 cm^2 area) were filled with 10–15 cm of sediment for the measurement of sediment permeability by the constant head method (Klute and Dirksen, 1986). Sub–samples were taken with 5 mL cut–off syringes and used for the determination of porosity (weight loss by drying). Sediment reactivity, approximated by the rate of oxygen consumption, was determined by injecting oxygenated water into the sediment at locations close to the optode but far from the organisms and subsequently measuring

116 porewater oxygen concentrations in 10 s intervals until all oxygen was consumed (which took 1-
117 5 min, depending on the sediment type). The volumetric rate of sedimentary oxygen
118 consumption, K_{OX}, expressed in micromoles of O_2 per volume of sediment (L_s) and time (µmol
119 O_2 L_s^{-1} min^{-1}), was then estimated as the initial rate of decrease in the measured porewater O_2
120 concentrations multiplied by sediment porosity (Polerecky *et al.*, 2005; Volkenborn *et al.*, 2010).
121
122 ***a. Study species and experimental setup***
123 *Macomona liliana* is a common bivalve in New Zealand intertidal sandflats (Roper *et al.*, 1992),
124 where it lives up to 10 cm below the sediment surface (Powell, 1979). Twenty large individuals
125 (shell length of 4.1–5.0 cm) were collected in February 2010 from an intertidal sandflat near the
126 northern entrance of Tauranga Harbour, North Island, New Zealand (37º27.77'S 175º57.90'E)
127 and four small individuals (shell length of 2.3–2.4 cm) were collected nearby, west of Tuapiro
128 Point (37º29.37'S 175º57.0'E). For porewater pressure measurements, circular containers (11.1
129 cm diameter and 10.5 cm deep for large individuals; 17.5 cm diameter and 11 cm deep for small
130 individuals) were filled with sediment and immersed in running artificial seawater (Red Sea Salt,
131 Red Sea Aquatics Ltd, Eilat, Israel) (31–34 ‰ salinity). For measurements with large individuals
132 eight containers were filled with either muddy sand or sandy sediment. For measurements with
133 small individuals we only used muddy sand sediment. Each container was equipped with a
134 pressure sensor at approx. 8 cm depth. Time–lapse photographs (every 15 s) were taken from
135 above with SLR cameras with flash (Nikon D200 and D300). Experiments were done at a
136 temperature of 17–19°C under ambient light and lasted for 6 days. Oxygen imaging was done on
137 four *M. liliana* individuals, incubated in narrow aquaria (20 cm × 4.5 cm surface, 20 cm deep).
138 Two of these aquaria were filled to a depth of approximately 15 cm with muddy sand and sandy

139 sediment, respectively. Overlying water was exchanged at a rate of 100 mL min^{-1}, resulting in
140 complete exchange every 5 min. Each aquarium was equipped with a pressure sensor that was
141 inserted from above to about 8 cm depth, and with oxygen sensitive foils (20 cm × 20 cm) that
142 were glued to the inside of both large walls. Incubations were done in the dark for 7 days at 20–
143 23°C. Oxygen images were taken simultaneously from 2 aquaria every 15 s and time–lapse
144 photographs were taken from above 5 s after each optode image. The aquaria were exchanged
145 and rotated opportunistically in order to capture periods with tellinids irrigating close to the
146 optode.
147
148 *Macoma nasuta* is abundant in intertidal flats in the eastern North Pacific Ocean, where it
149 burrows 10–20 cm deep into the sediment (Levinton, 1991; Meyerhöfer, 1985). Six specimens
150 with a shell length of 4.7–5.2 cm were collected in April 2010 from the mid to high intertidal of
151 False Bay, Washington, USA (48º29.35'N, 123º4.03'W). Individuals were incubated in six
152 square aquaria (10 × 10 cm surface, 20 cm deep), filled to approximately 15 cm with either
153 muddy sand or sandy sediment. One wall of each aquarium was equipped with an oxygen
154 sensitive foil (10 cm × 20 cm) and pressure sensors were deployed from above at approx. 8 cm
155 depth. Overlying water (from Friday Harbor Laboratories seawater system) was exchanged at
156 100 mL min^{-1}, resulting in a complete exchange approx. every 5 min. Oxygen images from the
157 side were taken simultaneously from the six aquaria and top–down time–lapse flash–illuminated
158 photographs were taken with a 5 s delay. Measurements were done over a period of 4 days in the
159 dark at a temperature of 12–14°C and a salinity of 34 ‰.
160

161 *Macoma balthica* is a cosmopolitan nearshore bivalve abundant in intertidal areas of the northern
162 parts of the Atlantic and Pacific Oceans. Porewater pressure measurements and time–lapse
163 photography were done in Germany in May 2007 and August 2011. Four individuals with shell
164 lengths between 1.8–2.0 cm were collected from a mid–intertidal sandflat in Königshafen, Sylt,
165 Germany (55º02.21'N, 8º24.53'E) and individuals were held in sediment–filled 1 L beakers (in
166 2007) or 5 L buckets (in 2011) immersed in running seawater from the Wadden Sea Station
167 seawater system. Measurements were done over 6 days at a temperature of 15–18°C and a
168 salinity of 33–35 ‰. Oxygen imaging was done in Finland in August 2011. Six individuals of *M.*
169 *balthica* (~1.6 cm shell length) were collected from a subtidal location near the Tvärminne
170 Zoological Station (59º50.60'N, 23º15.71'E). The set–up was the same as in the *M. nasuta*
171 experiments (see above). Measurements were done in the dark at 12–15°C and a salinity of 6 ‰.
172
173 ***b. Porewater pressure analysis***
174 Porewater pressure data were analyzed with respect to time allocation to feeding activity,
175 burrowing, and inactivity for each individual. Intervals of inactivity were defined as periods
176 without porewater pressure dynamics for >30 min. Burrowing episodes were defined as time
177 intervals with high magnitude pressure oscillations with intermittent sediment pressurization,
178 where there were < 20 min between subsequent intervals of high magnitude pressure oscillations.
179 The first and last high magnitude pressure pulses were used as start and end points to define a
180 burrowing episode. For periods of deposit–feeding the average durations of pressurized (T_{PUMP})
181 and non–pressurized (T_{REST}) intervals and the average frequencies of feeding bouts were
182 determined for each individual. Feeding bouts were defined as distinct if separated by a > 20 s
183 gap. Effects of the sediment type on these measures of hydraulic activity were tested for each

184 species by one–way factorial ANOVA. For *Macomona liliana* the effect of tellinid size on the
185 temporal patterns in hydraulic activity was additionally tested by a one–way factorial ANOVA.
186
187 ***c. Transport-reaction modeling***
188 To study the spatial and temporal dynamics of O_2 in an intermittently bioirrigated sediment, a
189 transport-reaction model was set up in COMSOL 4.3, a finite–element modeling environment.
190 The 2D axisymmetric model domain consisted of a cylinder (radius 20 cm, sufficiently large to
191 minimize boundary effects) with the top 2 cm filled with water and the bottom 20 cm with
192 sediment. The mesh consisted of approximately 5500 finite elements with side lengths between
193 <1 mm near the injection pocket and the sediment water interface and 6 mm in regions with low
194 flow and small concentration gradients. A spherical injection pocket with a radius of 0.2 cm was
195 positioned on the central symmetry axis 5.75 cm below the sediment surface. The transport of
196 the overlying water and porewater was modeled using COMSOL's implementation of Navier–
197 Stokes and Brinkman equations describing free flow in an isotropic porous media (Le Bars and
198 Grae Worster, 2006), accounting for pressure gradients and viscous forces but neglecting inertial
199 terms. As a solver we used the sparse direct solver MUMPS (http://graal.ens-lyon.fr/MUMPS).
200 The top of the domain was set as open (zero normal stress), and the normal flow at the bottom
201 and vertical domain boundaries was set to zero. Intermittent irrigation was modeled by imposing
202 the fluid velocity at the injection boundary to values that varied between zero (during the resting
203 interval T_{REST}) and the ratio of the instantaneous volumetric pumping rate and the surface area of
204 the injection pocket (during the pumping interval T_{PUMP}). Permeability of 5×10^{-12} m^2 and
205 porosity 0.45 were used in all simulations. Because irrigation was implemented by imposing

flow velocity rather than pressure at the inlet boundary, the flow velocity field and the results derived from it were not affected by this choice of sediment permeability.

Pumping rates of tellinid bivalves for model parameterization were derived from the literature. For *Macoma nasuta* of comparable sizes to those used in our experiments (5.0 cm shell length), Meyerhöfer (1985) measured instantaneous pumping rates of 1.8 mL min^{-1} with thermistor probes. Based on this instantaneous pumping rate, and given the proportional time of active irrigation by *M. nasuta* measured in this study (7 irrigation bouts h^{-1}, 5 min duration; see Results), time–integrated pumping rates would be around 1.1 mL min^{-1}, which is in the range of pumping rates estimated with the "clambox" when averaged over 12 min intervals (Specht and Lee, 1989). Assuming the *Macoma nasuta* dry weight versus instantaneous pumping rate relationship estimated by Meyerhöfer (1985), and the size versus dry weight relationship found by Gallucci and Hylleberg (1976), we estimated the instantaneous pumping rates for the size classes used in our experiments to be 1.8, 1.6, 0.43, and 0.35 mL min^{-1} for *M. nasuta*, large and small *M. liliana*, and *M. balthica*, respectively. In additional simulations exploring the relationship between pumping rates and oxic sediment volumes, instantaneous pumping rates were varied between 0.1 and 3 mL min^{-1}.

O_2 concentrations in the porewater, denoted as C, were computed using

$$\phi \frac{\partial C}{\partial t} = \nabla \cdot \left(D \nabla C\right) - \vec{u} \cdot \nabla C + R \qquad (1)$$

where $\vec{u}$ is the advection velocity field (m s^{-1}), ϕ is porosity, and D (in m^2 s^{-1}) parameterizes diffusion when in the sediment ($D = \phi/(1\text{-}2\times\ln(\phi))\times D_{mol}$, with $D_{mol} = 1.9 \cdot 10^{-9}$ m^2 s^{-1} ; Schulz, 2000) and dispersion when in the overlying water ($D = D_{mol} + 0.4 \cdot \nu/363 \cdot (z \cdot u^*/\nu)^3$, where ν is the

229 kinematic viscosity (10^{-6} m^2 s^{-1}), u* is shear velocity and z is the distance from the sediment–
230 water interface; Boudreau, 2001). The shear velocity was set to 10^{-5} m s^{-1}, which was sufficient
231 to establish a homogeneous O_2 concentration distribution in the overlying water; its value did not
232 significantly affect the burrow-associated oxic sediment volume discussed below. Hydrodynamic
233 dispersion in the sediment was neglected because it plays only a minor role at low flow velocities
234 (Meysman *et al.*, 2006). The net O_2 consumption rate *R* was set to 0 in the overlying water and
235 was modeled as $-K_{OX} \times C / (K_M+C)$ in the sediment, where K_{OX} is the maximum sedimentary
236 oxygen consumption rate (see above) and K_M is the half–saturation constant. In muddy sands,
237 K_{OX} values are typically in the range of 5–30 μmol L_s^{-1} min^{-1} (Glud et al. 2003; Volkenborn *et*
238 *al.*, 2010). In more muddy sediments, they may exceed 50 μmol L_s^{-1} min^{-1} (e.g., Volkenborn *et*
239 *al.*, 2012), and are typically <5 μmol L_s^{-1} min^{-1} in highly permeable sands (Billerbeck *et al.*,
240 2006; Werner *et al.*, 2006; Volkenborn *et al.*, 2012). Model simulations used K_{OX} values in the
241 range from 2.25 to 45 μmol L_s^{-1} min^{-1}, thus covering the range found in natural sediments. The
242 half–saturation constant K_M was set to 1 μM, with comparable results achieved when setting it to
243 10 μM (not shown) which is in the range of K_M values used in previous studies (e.g., Van
244 Cappellen and Wang, 1995). In all simulations, a no flux condition was imposed at the bottom
245 and side of the domain, and O_2 concentration of 220 μM was imposed at the top of the domain,
246 whereas in the injected water it was set to 88 μM, consistent with the maximal porewater O_2
247 concentrations detected at the aquarium wall in our experiments (typically around 40% air
248 saturation). This reduction in O_2 can be mostly attributed to the respiratory O_2 uptake by the
249 pumping organisms.

3. Laboratory results

a. Tellinid behaviors and related porewater pressure waveforms. All three tellinid species engaged in a range of hydraulic activities that caused behavior–specific porewater pressure waveforms. An exemplary pressure record from *Macomona liliana* is shown in Figure 1. Most of the time, all 3 species were surface–deposit–feeding (videos 1–3 in the appendix). Episodes of deposit–feeding lasted from several hours to a few days and were characterized by intermittent irrigation as indicated by frequent alternations of pressurized and non–pressurized intervals (Fig. 1). From time to time tellinids relocated their excurrent siphons, which could be seen in time–lapse images as a change in the location of particle movement and accumulation of fecal pellets at the sediment surface. Movements of the excurrent siphon occurred while the sediment was pressurized and caused short positive pressure pulses at typical frequencies of 2 pulses min^{-1} (Fig. 1C). Movements of the incurrent siphon were associated with short positive or negative pressure pulses around the hydrostatic pressure baseline. Deposit–feeding was accompanied by frequent sediment blow–outs through the incurrent and excurrent siphons, i.e. pseudofeces expulsions and defecations, respectively, both causing very similar short negative or positive pressure pulses (<4 s decreasing pressure, followed by an active recovery or sediment–dependent pressure recovery over 2–7 s). Burrowing caused substantial sediment movement, and was characterized by large positive and negative pressure pulses (Fig. 1B). The frequencies and durations of hydraulic activities varied among species (Figs. 2 and 3; Table 1). However, for all of them, the time–integrated pressures (pressure amplitude × duration) during the pulses associated with feces or pseudofeces expulsions were typically <5 % of the pressures integrated over one irrigation bout. Thus, though large in amplitude, the short duration of the pressure

273 pulses associated with feces and pseudofeces expulsions suggests little contribution of these
274 behaviors to the transport of porewater by the bivalves, which is consistent with findings for
275 arenicolids (Wethey *et al.,* 2008). Thus, we have focused the analysis on the intermittent
276 porewater pressurization during deposit–feeding, since this behavior was the most important in
277 terms of time allocation (Table 1) and porewater advection.
278
279 ***b. Species–specific irrigation patterns.*** Analysis of the pressure records revealed that the average
280 durations of pumping (T_{PUMP}) and resting (T_{REST}) differed among tellinid species and size classes
281 (Fig. 2, Table 1) The temporal irrigation patterns of individuals were characterized by a
282 substantial variation around the individual means. On average, the standard deviation of T_{PUMP}
283 and T_{REST} of individuals was 40% of the mean duration (Fig. 3).
284
285 The large *Macomona liliana* specimens were hydraulically active 94% of the time (n=16
286 individuals, 8 in mud, 8 in sand over 5 days). 88 (± 4) % of the time these individuals were
287 deposit-feeding. Feeding episodes were characterized by intermittent porewater pressurization,
288 with 8.3 (± 2.5) min of pressurization separated by 10.0 (± 1.8) min intervals of no hydraulic
289 activity (mean and SD of 16 individuals with 50–317 bouts analyzed per individual). This
290 corresponded to 3.3 (± 0.5) feeding bouts h^{-1} and pressurization of the sediment during 45 (±10)
291 % of the time while feeding. Sediment type had no significant effect on the durations of
292 pressurized ($F_{1,14}$=0.94; p=0.35) and non–pressurized ($F_{1,14}$=1.14; p=0.30) intervals or feeding
293 bout frequencies ($F_{1,14}$=0.11; p=0.74). Feeding activity by the small *M. liliana* specimens (n=4,
294 all in muddy sand, 82 to 122 bouts analyzed per individual) was characterized by barely
295 significantly shorter pressurized (4.4 ± 1.0 min, $F_{1,10}$=4.8; p=0.051), significantly shorter non–
296 pressurized (6.7 ± 1.8 min; $F_{1,10}$=12.9; p=0.005) intervals, and significantly higher feeding bout

297 frequencies (5.6 ± 1.2 min; $F_{1,10}$=18.6; p=0.002) when compared to the larger conspecifics
298 feeding in the same muddy sediment type.
299
300 *Macoma nasuta* was hydraulically active 93% of the time (n=5 individuals over 3–4 days). After
301 the initial burrowing, they were actively deposit–feeding 83 (± 20) % of the time (mean and SD
302 of 5 individuals), with 2 individuals allocating a significant portion of the time to suspension
303 feeding (28% and 19%). While deposit–feeding, the incurrent siphon was continuously moving
304 around, ingesting surface sediment. Deposit–feeding was characterized by 5.0 (± 1.0) min of
305 pressurization separated by intervals of 3.7 (± 1.1) min (n=5 individuals, with 94–167 feeding
306 bouts analyzed per individual). The average frequency of feeding bouts was 7.1 (± 1.4) h^{-1}.
307 Burrowing accounted for 2.4 (± 3) % of the time budget and burrowing episodes lasted 68 (± 20)
308 min. 3 of 6 individuals did not burrow at all after the episode of initial burrowing.
309
310 *Macoma balthica* individuals were small compared to the other tellinid species and the
311 magnitude of porewater pressurization was very small most of the time. Time allocation of
312 deposit–feeding was therefore determined from time–lapse photography. Over the 6–7 days of
313 observation the two individuals were actively feeding during 57% and 45% of the time. Feeding
314 occurred in bouts of 2.3 (± 0.2) min duration separated by intervals of 1.7 (± 0.2) min (78–197
315 bouts of 3 individuals analyzed). The feeding bout frequency was 15.1 (± 0.2) h^{-1}. Burrowing
316 occurred 0.62 (± 0.25) times per 24 h and lasted 12.9 (± 7.6) min.
317
318 ***c. Linking tellinid behaviors and oxygen dynamics.*** Over the course of the measurements, seven
319 of the 28 tellinid individuals positioned their excurrent siphons for some hours close to the

oxygen sensitive foil. While feeding, the sediment was intermittently supplied with oxygen. Oxygen dynamics were directly related to porewater pressurization, with oxygen concentrations increasing during pressurized and decreasing during non–pressurized intervals (Fig. 4). Oxic and anoxic intervals typically alternated on the scale of minutes in synchrony with the pressure records, and maximal oxygen concentrations were typically around 40% air saturation. Sometimes, as a result of water injection occurring at some distance from the optode, the detection of oxygen by the optode was delayed relative to the onset of porewater pressurization (Fig. 4A).

The differences in feeding bout frequencies and interval durations (Table 1; Fig. 2) caused species–specific oxygen dynamics in the sediment (Figs. 4, 5; Appendix video 4). For *M. liliana*, the oxygen delivered during feeding bouts was typically entirely consumed during the resting periods, and oscillations from oxic to anoxic and back to oxic conditions occurred at frequencies of < 3 times per hour, with oxic and anoxic periods typically lasting around 10 min (Figs. 4, 5). With *M. nasuta* oscillations between oxic and anoxic conditions occurred more frequently (up to 6 h^{-1}), congruent with the higher feeding bout frequencies documented by porewater pressure sensing for this species (Table 1). In the one occasion when a *M. balthica* specimen irrigated close to the optode, oxygen was present almost continuously, reflecting incomplete oxygen depletion during the short resting period between irrigation bouts.

4. Modeling intermittent bioadvection and O_2 dynamics

Based on the irrigation patterns determined with porewater pressure sensing, the size–specific instantaneous pumping rates from the literature and the oxygen concentrations of the injected

water determined with planar optode imaging, we modeled the dynamics of the oxic sediment volume (V_{O2}, defined as the volume of sediment with porewater O_2 concentrations >2 μM and depths >1 cm, i.e., below the depth to which O_2 penetrates by diffusion from the overlying water in our conditions) for the three species at 3 different sediment reactivities (Fig. 6). These reactivities correspond approximately to the range of sediments types that tellinids inhabit - from permeable clean sands to low permeability muddy sands.

a. Intermittent irrigation by tellinids. There was an increase in V_{O2} during each irrigation bout and a decrease after the irrigation stopped. Because of the long time intervals between irrigation bouts, the injection pocket of *Macomona liliana* experienced oxic to fully anoxic oscillations regardless of their oxygen consumption rates (Fig. 6A). For *Macoma nasuta*, model simulations predicted oxic-anoxic oscillatory conditions only for sediment with high and intermediate reactivity (Fig. 6B). For *Macoma balthica* oxygen was entirely consumed between subsequent irrigation bouts only in highly reactive sediments, while in sediments of intermediate and low reactivity portions of the irrigated pocket remained oxic due to the short intervals between subsequent irrigation intervals (Fig. 6C). Thus, the spatio-temporal patterns of oxygen distributions largely depend on the species- and size-specific irrigation patterns in relation to the sedimentary oxygen consumption rates.

b. Spatial extent of oxygenation. Model simulations showed that the maximal volume of the oxic sphere, V_{O2max}, depends on both the instantaneous pumping rate, Q, and the sediment reactivity, K_{OX} (Fig. 7). A relationship between these quantities derived from the model simulations was $V_{O2max} = m \times Q / K_{OX}$,, where the proportionality constant m = 81.5 μM (Fig. 8).

This relationship is consistent with the idea that, at steady state, the amount of oxygen injected into the sediment per unit time ($Q \times O_2^{injected}$, where $O_2^{injected}$ is the oxygen concentration in the injected water) is equal to the rate at which O_2 is consumed in the oxic sediment volume. For a low K_M value (1 μM), the rate of O_2 consumption in the sediment is approximately constant and equal to K_{OX} for a wide range of relevant O_2 concentrations. Therefore, the consumption rate can be approximated by $V_{O2max} \times K_{OX}$,, resulting in

$$V_{O2max} \approx (Q \times O_2^{injected}) / K_{OX}. \quad (2)$$

Indeed, $O_2^{injected}$= 88 μM in this expression closely approximates the proportionality constant m = 81.5 μM derived from the model results. The small difference, attributed to the combined effects of neglecting diffusive transport, neglecting reaction kinetics at low O_2 concentrations, and the use of a 2 μM threshold for defining oxic sediment, indicates that the role of these effects is minor.

Our experimental data support this estimate for the oxic sediment volume. For $O_2^{injected}$ = 88 μM, K_{OX} = 16 μmol L_s^{-1} min^{-1}, and Q = 1.6 mL min^{-1}, Eq. 2 predicts a V_{O2max} of 8.8 cm^3. Under these conditions we detected an intermittently oxic area of 4 cm^2 when *M. liliana* was injecting water into the sediment close to the O_2 sensitive foil (Fig. 5). The ratio of the predicted (intermittently) oxic volume and the measured oxic area suggests that the detected area extended roughly 2.2 cm into the sediment away from the oxygen sensitive foil, which seems reasonable, given the uncertainties with respect to the shape of the oxic pocket (e.g. we do not know if we are seeing a cross–section through the center or through the outer part of the oxic pocket).

c. Temporal dynamics of oxygenation. Given the intermittent irrigation activity of tellinids, the questions arise as to whether V_{O2max} is reached over a single irrigation bout and whether the oxic pocket becomes fully anoxic between subsequent irrigation bouts.

The metric of interest for redox oscillation is the fraction of V_{O2max} that is reached after a given duration of pumping and not the size of V_{O2max}. The size of V_{O2max} depends on the instantaneous pumping rate (Fig. 8; Eq. 2); however, the fraction of V_{O2max} reached after a given duration of pumping does not (Fig. 9 A and B). The fraction of V_{O2max} that is reached after a given duration of pumping does depend on K_{OX} (Fig. 9A). Furthermore, as shown by the solid lines in Fig. 9A, the increase of V_{O2} towards V_{O2max} is well approximated by

$$V_{O2} / V_{O2max} \approx A \times \{1-\exp[(-K_{OX} \times T_{PUMP}) / (O_2^{injected} \times \phi)]\} + B, \quad (3a)$$

where T_{PUMP} is the time since the start of the pumping activity. The fitting parameters A and B depend on K_{OX} approximately as

$$A \approx a_0 + a_1 K_{OX} + a_2 K_{OX}^2, \quad (3b)$$

$$B \approx b_0 + b_1 K_{OX}, \quad (3c)$$

where $a_0 = 1.444$, $a_1 = -3.985 \times 10^{-3}$ L_s min μmol^{-1}, $a_2 = 5.16 \times 10^{-5}$ L_s^2 min^2 μmol^{-2}, $b_0 = -0.01$, $b_1 = 1.06 \times 10^{-3}$ L_s min μmol^{-1}. The regression coefficient R^2 for equation 3b is 0.98 and 0.99 for equation 3c. Model simulations also show that the time required for the volume of oxic sediment to increase from zero to 95% of V_{O2max}, denoted as T_{O2max}, is also independent of the instantaneous pumping rate but increases with decreasing values of K_{OX} (Fig. 9C). This relationship is well approximated by

$$T_{O2max} \approx O_2^{injected} \times \phi / K_{OX}. \quad (4)$$

411 Based on the average durations of T_{PUMP} for the tellinids used in our experiments (Table 1),
412 equation 4 allows prediction of the K_{OX} value above which a specific tellinid species and size
413 class will establish 95% of V_{O2max} over the course of a single irrigation bout (see dotted
414 horizontal lines in Fig. 9C). For example, at $K_{OX} > 20$ µmol L_s^{-1} min^{-1} even the short pumping
415 intervals of *Macoma balthica* will establish 95% of V_{O2max}, while at $K_{OX} <5$ µmol L_s^{-1} min^{-1}
416 none of the tellinids in our experiments would be, on average, pumping sufficiently long to reach
417 95% of V_{O2max}. Similarly, equations 3a-c allow prediction of the fraction of V_{O2max} reached by
418 pumping water with oxygen concentration $O_2^{injected}$ into permeable sediment of a given reactivity
419 K_{OX} for a given interval T_{PUMP}, provided that the injection pocket at the start of pumping is fully
420 anoxic. For example, for $O_2^{injected}$ = 88 µM, the volume of the oxic sediment induced by pumping
421 for 2 min would be 50% of V_{O2max} for K_{OX}=9 µmol L_s^{-1} min^{-1} but 80% of V_{O2max} for K_{OX}=18
422 µmol L_s^{-1} min^{-1} (Fig. 9A). It should be noted that these approximations are valid only for such
423 combinations of values of K_{OX}, T_{PUMP} and $O_2^{injected}$ that the predicted ratio V_{O2} / V_{O2max} falls
424 within the range 1% to 95%.
425
426 Model simulations show that the fraction of V_{O2max} that is still oxic after a given duration of no
427 irrigation (T_{REST}) does not depend on the instantaneous pumping rate but only on K_{OX} (Fig. 9B),
428 and that it is well approximated by

429 $$V_{O2} / V_{O2max} \approx A\times \{1 - (T_{REST} \times K_{OX}) / (O_2^{injected} \times \phi)\} + B \quad (5)$$

430 The fitting parameters A and B depend on K_{OX} approximately as Eq 3b and Eq 3c, where a_0 =
431 1.005, $a_1 = 1.573 \times 10^{-4}$ L_s min μmol^{-1}, $a_2 = 2.62 \times 10^{-5}$ L_s^2 min^2 μmol^{-2}, $b_0 = 0.012$, $b_1 = -2.93 \times$
432 10^{-3} L_s min μmol^{-1}. The regression coefficient R^2 is 0.99 for both.
433

Likewise, the time it takes for the oxic sediment to decrease from V_{O2max} to a volume < 1 % of V_{O2maxs}, denoted as T_{O2zero}, is independent of V_{O2max}, depends only on K_{OX} (Fig. 9D), and is well approximated by (Fig. 9D)

$$T_{O2zero} \approx O_2^{injected} \times \phi / K_{OX}. \quad (6)$$

Thus, based on the average durations of T_{REST} for the tellinids used in the experiments (Table1), equation 6 allows prediction of the K_{OX} value above which oxygen is completely consumed in the course of an average resting interval for any of the tellinid species and size classes (see dotted lines in Fig. 9D). For example, at $K_{OX} > 23$ µmol L_s^{-1} min^{-1} even the short resting interval of *Macoma balthica* is sufficiently long to allow complete oxygen depletion, while at $K_{OX} < 3.7$ µmol L_s^{-1} min^{-1} none of the tellinids in our experiments would be, on average, resting sufficiently long to allow complete oxygen depletion in the injection pocket. Similarly, equation 5 allows prediction of the fraction of V_{O2max} reached in a sediment of a given reactivity K_{OX} after resting for a given interval T_{REST}, provided that $V_{O2} = V_{O2max}$ at the start of resting. For example, after 2 min of resting the fraction would be about 55% for $K_{OX} = 9$ µmol L_s^{-1} min^{-1} but only about 10 % for $K_{OX} = 18$ µmol L_s^{-1} min^{-1} (Fig. 9B).

5. Discussion

a. Intermittent irrigation and redox oscillations in permeable sediments. Bioturbation creates heterogeneous and dynamic geochemical conditions in sediments (Aller, 1994), but our ability to quantify and predict the spatio–temporal dynamics is still limited, especially in advection–dominated systems. In these environments infaunal activities can be a predominant driver of porewater transport (Meysman *et al.*, 2005; Volkenborn *et al.*, 2007; Wethey *et al.*, 2008) that

457 brings oxygenated fluids into contact with suboxic or anoxic sediment. Models of continuous
458 bioirrigation adequately predict gradients in porewater solutes (Aller, 1980; Na *et al.*, 2008), but
459 they do not allow characterization of the temporal dynamics of the geochemical conditions
460 associated with infaunal activity. Intermittent irrigation is not unique to tellinids, but is
461 characteristic for many different types of infauna, such as arenicolid polychaetes (Kristensen,
462 2001; Timmermann *et al.*, 2006; Volkenborn *et al.*, 2010), nereid polychaetes (Foster–Smith,
463 1978; Kristensen, 2001; Pischedda *et al.*, 2012), terebellid polychaetes (Aller and Yingst 1987),
464 thalassinid crustaceans (Forster and Graf, 1995; Volkenborn *et al.*, 2012) or chironomid insect
465 larvae (Polerecky *et al.*, 2006; see also review by Riisgård and Larsen, 2005). Thus, periodic
466 oxygen supply is the rule rather than the exception in bioturbated sediments. The resulting
467 spatial–temporal patterns in redox conditions are largely driven by (i) durations and frequencies
468 of active irrigation intervals, (ii) instantaneous pumping rates, and (iii) sediment reactivity, e.g.,
469 sedimentary oxygen consumptions rates. Given the potential effects of redox oscillations on
470 organic matter mineralization as well as the probable interruption of anoxic or oxic pathways as
471 the oscillation occurs, it is critical to explore the factors constraining stable or oscillatory redox
472 conditions.
473
474 The instantaneous pumping rates of individuals constrain the maximal sediment volumes
475 (V_{O2max}) that are supplied with oxygen (Figs. 7B and 8A), but they do not affect the temporal
476 dynamics of the intermittently oxic pockets. Model simulations indicate that the wax and wane
477 of the oxic pockets are solely governed by the temporal irrigation patterns (T_{PUMP} and T_{REST}), the
478 sedimentary oxygen consumption rates K_{OX} , and the oxygen concentrations in the irrigation
479 water (Fig. 7A). The model results (Figs. 8 and 9) and the analytical approximations (equations

2-6) allow predictions of the volumes of sediment that are supplied with oxygen as well as of the relative proportion of sediment that experiences oscillatory or continuously oxic conditions for a wide range of sediment types and temporal irrigation patterns.

Overall, model simulations suggest that over a wide range of sediment types (i.e., with K_{OX} >23 µmol L_s^{-1} min^{-1}) the volumes of subsurface sediment pockets that become oxic as a result of intermittent irrigation activity by the studied tellinids are similar to those derived from continuous irrigation models, and that the entire pockets switch between oxic and anoxic conditions during an average T_{PUMP}-T_{REST} cycle. In a typical muddy sand sediment (ϕ = 0.45; K_{OX} =25 µmol L_s^{-1} min^{-1}; Volkenborn *et al.*, 2010) with 50 tellinids m^{-2}, the intermittent injection of water with an instantaneous pumping rate of 1.6 mL min^{-1} $ind.^{-1}$ (Meyerhöfer, 1985) with an oxygen concentration of 88 µM will result in a sediment volume of approximately 280 cm^3 m^{-2} that oscillates between oxic and anoxic conditions several times per hour.

However, short durations of T_{PUMP} and T_{REST} in combination with low reactivities of the sediment make it more likely that at the end of T_{PUMP} the oxic sediment pocket is not in steady-state and that oxygen is not fully consumed at the end of T_{REST} (Figs. 9 A and B). Under these conditions, different irrigation patterns with similar time-integrated pumping rates may have very different geochemical consequences. For example, in a sediment with K_{OX} = 18 µmol L_s^{-1} min^{-1}, irrigation patterns of T_{PUMP} = 3 min and T_{REST} = 3 min will result in an oscillating sediment volume of V_{O2max}, whereas for T_{PUMP} = 1 min and T_{REST} = 1 min the maximal volume of oxygenated sediment will be about 50% smaller and < 50% of this volume will be oscillating (Fig. 9A and B).

Given the variability of T_{PUMP} for the studied tellinid individuals (Fig. 3), the maximum volume of oxygenated sediment (V_{O2max}; see Eq. 2) will not be established during some of the shorter irrigation bouts (compare Figs. 3 and 9), which is congruent with our observation that oxic-anoxic oscillations are less frequent in the outer region of the oxygenated pockets (see images of F_{REDOX} for *M. nasuta* and *M. liliana* in Fig. 5). Similarly, given the temporal variability of T_{REST} (Fig. 3), some intervals of resting will be too short for the sediment to become fully anoxic before the onset of the next pressurization interval. This is apparent in the optode imagery for *M. nasuta* during minute 20 to 35, when T_{REST} intervals were short, in contrast to minute 45 to 60 min, when T_{REST} intervals were longer and there was an anoxic interval between the subsequent feeding bouts (Fig. 4).

The tellinids were all engaged in the same suite of hydraulic behaviors, but the temporal patterns of these activities and, consequently, their geochemical impact varied among species and size classes. Besides species-specific aspects it was the size of the tellinids that constrained the duration of T_{PUMP} and T_{REST}. Very likely, the smaller gills provide less space to accumulate particles during deposit–feeding, which forces smaller individuals to expel particles more frequently. Given that the geochemical dynamics are directly linked to the durations of pumping and resting intervals, the geochemical signature of an individual is likely to change also as a result of behavioral response to the environmental conditions. In our experiments, tellinids were deposit–feeding most of the time (Table 1), but tellinid behavior is known to vary depending on the environmental conditions. Deposit–feeding dominates in fine sediments (Olafson, 1986) and at low water flow velocities (Levinton, 1991), while the time spent suspension feeding increases

526 at high population densities (Marinelli and Williams, 2003) and high food availability in the
527 water column (Hummel, 1985; Lin and Hines, 1994). *Macoma balthica* shows reversible
528 morphological changes in response to changes in food conditions, with smaller gill (particle
529 collection) to palp (particle sorting) ratios in finer sediments (Drent *et al.*, 2004). The location of
530 subsurface water injection can also change with environmental conditions. The burrowing depth
531 of tellinids is affected by animal size, length of the incurrent siphon, sediment type, season, and
532 the presence of predators (Zwarts and Wanink, 1989; Tallqvist, 2001). In our narrow aquaria the
533 excurrent siphons were often located in the upper 4 cm of sediment, and it may well be that the
534 constrained conditions in ant–farm and container settings as well as the relatively short duration
535 of experiments may have limited burrowing depth.
536
537 We did not find a significant difference in hydraulic activity in response to sediment type, but for
538 some individuals we occasionally observed periods of irrigation without obvious uptake of
539 sediment particles. The duration of sediment pressurization increased during such periods. For
540 example, for one *M. nasuta* individual that was pumping without particle uptake, the durations of
541 irrigation and resting intervals increased from 5.2 min and 4.9 min while deposit–feeding (Table
542 1) to 20 min and 10 min, respectively (mean of 26 bouts over a 5 hour period). Model
543 simulations predict that at, e.g., $K_{OX} = 4.5$ µmol L_s^{-1} min^{-1} such a change in the irrigation pattern
544 will result in a 1.7 fold larger oxic pocket (Fig. 9A), and instead of continuously oxic conditions
545 within 40 % of the pocket, the entire volume will switch between oxic and anoxic conditions
546 (Fig. 9B). Thus, environmental factors that are known to affect temporal infaunal activity
547 patterns, such as temperature (Stief *et al.*, 2010), oxygen concentrations (Dales *et al.*, 1970;
548 Mangum and Burnett, 1975), organism densities (Marinelli and Williams, 2003), flow velocities

549 (Levinton, 1991), food availability in the water column (Hummel, 1985; Lin and Hines, 1994),
550 the presence of predators and injury (Kamermans and Huitema, 1994), or a combination of these
551 factors (e.g., Kolar and Rahel, 1993), are also likely to influence the magnitude and dynamics of
552 sediment oxygenation. The relatively low variability in the means of T_{PUMP} and T_{REST} in tellinids
553 of the same species and size class (Fig. 3, Table 1) suggests that the observed irrigation patterns
554 were robust representatives of species- and size class- specific activity patterns in our
555 experimental settings. However, given the responsiveness of tellinids to a wide range of
556 environmental variables, such external factors may, via their impact on infaunal behavior,
557 ultimately also impact the geochemical dynamics in the sediment.
558
559 ***b. Simplifying model assumptions.*** Model simulations enabled us to show that the interplay
560 between biological parameters (instantaneous pumping rates, temporal patterns of irrigation,
561 efficiency of respiratory O_2 uptake by the animal) and the sediment characteristics (sedimentary
562 oxygen consumption rates, sediment porosity) result in specific oxic-anoxic oscillatory
563 conditions in the sediment. It should be noted that O_2 concentrations in the irrigated water as
564 well as porosity of the sediment lie within a relatively narrow range compared to instantaneous
565 pumping rates and sedimentary oxygen consumption rates, which both may vary over 2 orders of
566 magnitude and more. Thus, it is the volumetric instantaneous pumping rate (related to organism
567 size and species), the O_2 consumption rate of the sediment and the duration of irrigation and
568 resting intervals that constrain the oxygenated sediment volume (Figs. 8 and 9). In model
569 simulations we did not account for the spatial – and maybe even more importantly the temporal –
570 variability of K_{OX}. From repeated injections of oxygenated water close to the planar optode and
571 measurements of subsequent decays of oxygen in time, we know that over the first few injections

572 K_{OX} typically decreases, which can be attributed to the initially rapid oxidation of a highly
573 reactive pool of reduced compounds (Polerecky *et al.*, 2005). With repeated injections of oxic
574 water over the course of hours to days, K_{OX} is expected to change as a result of changes in
575 microbial activity and abundance, as well as changes in sediment porosity and organic matter
576 content. Organic rich fecal pellets, for example, accumulate around the injection pocket and are
577 characterized by high nitrifying activity (Henriksen *et al.*, 1983), which will alter oxygen
578 consumption rates and may relate to the repositioning of the bivalve on timescales of days.
579 Dynamic changes of K_{OX} around the injection pockets may have been responsible for some of
580 the mismatches between planar optode measurements and model output data. For example, for
581 very comparable values of K_{OX} the steady-state oxic volume (V_{O2max}) was established for shorter
582 time intervals in one of our measurements (Fig. 4a: *M. liliana* at K_{OX} = 16 µmol L_s^{-1} min^{-1}) than
583 predicted from model simulations (Fig. 6A: *M. liliana* at K_{OX} = 18 µmol L_s^{-1} min^{-1}). Estimates of
584 K_{OX} from the oxygen decrease after this tellinid had stopped pumping during the time interval
585 shown in Fig. 4a varied between 8-10 µmol L_s^{-1} min^{-1}. Thus, K_{OX} was lower than our estimate
586 based on water injections in distant anoxic sediment and the model indeed predicted shorter
587 intervals of steady-state oxic sediment volumes at lower values of K_{OX} (Fig. 6).
588
589 K_{OX} varies also seasonally due to changes in temperature, organic content and microbial activity
590 (Glud *et al.*, 2003; Billerbeck *et al.*, 2006; Werner *et al.*, 2006). For example, Werner *et al.*
591 (2006) documented a 20-fold change in sedimentary oxygen consumption rates between summer
592 (K_{OX} ≈ 14 µmol L_s^{-1} min^{-1}) and winter (K_{OX} ≈0.7 µmol L_s^{-1} min^{-1}). As a consequence of such
593 variation in sediment reactivity, the geochemical signature of a species with a specific irrigation
594 pattern may change, e.g., from a mostly continuously oxic pocket at lower K_{OX} (i.e., in winter) to

a mostly oscillatory pocket at higher K_{OX} (i.e., in summer). Thus, due to the dynamic and heterogeneous nature of oxygen consumption rates predictions of (intermittently) oxic sediment volumes based on the (average) reactivity of the bulk sediment will only be as accurate as estimates of K_{OX} within this sediment volume.

Another crucial assumption in our model was homogenous sediment permeability. This resulted in close to spherical oxic pockets in the model. However, the optode data suggest that the tellinids frequently created rather vertical cylinders (Figs. 4, 5), suggesting locally enhanced upward movement of injected water. Visual observations as well as the porewater pressure data (Fig. 1) suggest that tellinids are capable of injecting water at much higher flow rates, e.g., during defecations. These "jets" can induce sedimentary cracks to the surface (Matsui *et al.*, 2011). Furthermore, fecal pellets accumulate over time around the injection pockets, which further alter not only the reactivity but also the physical characteristics of the sediment. Occasionally, we observed suboxic water exiting the sediment, especially when injection occurred at a relatively shallow depth. In concert, these phenomena are likely to impact the shape and size of the oxygenated pockets beyond the factors assessed in the numerical model and analytical expressions presented here.

6. Conclusions and perspectives

Intermittent irrigation by infaunal organisms has been shown to create geochemically dynamic zones in the sediment where oxic and anoxic conditions alternate on the scale of minutes (Volkenborn *et al.*, 2012). This study is a first attempt to integrate the intermittent nature of bioirrigation into a numerical transport-reaction model that allows an exploration of the related

redox dynamics. Model simulations as well as the simple analytical approximations derived from these simulations indicate that temporal irrigation patterns in concert with sedimentary oxygen consumption rates play an important role in constraining the intermittently or continuously oxic sediment volumes. Furthermore, the simulations predict that oscillatory rather than stationary redox conditions are prevalent in a wide range of sediments inhabited by tellinid bivalves.

We expect that the transient availability of oxygen in the sediment has significant implications for biogeochemical processes. Oxic–anoxic oscillations on the scale of days to weeks have been found to increase rates of organic degradation when compared to continuous oxic or continuous anoxic conditions (Aller, 1994; Sun *et al.*, 1993). Though insights into how microbial assemblages respond to fluctuating conditions are limited (Cravo–Laureau *et al.*, 2011), the higher efficiency in organic mineralization is thought to result from the activation of different microbial assemblages during oxic and anoxic conditions (Sun *et al.*, 1993). Here, we have shown that oxic–anoxic oscillations not only occur on the scale of hours to days, e.g., due to repositioning of excurrent siphons, but also on much shorter time scales, with oxic and anoxic conditions alternating up to six times per hour within these ephemeral oxic pockets (Figs. 4, 5). How microbial assemblages deal with these rapid changes is largely unexplored. For example, oxic–anoxic fluctuations on comparable short time–scales occur when oxic surface sediment is ingested by deposit–feeding infauna and is exposed to anoxic conditions within the digestive tract (Stief *et al.*, 2009). The residence time of the sediment in the gut is typically in the range of 30 min. It was found that this duration is not sufficient to allow complete denitrification, which resulted in significant release of nitrous oxides. Thus, rapid oscillations between oxic and anoxic conditions not only reduce the time during which aerobic mineralization can take place, they

may also affect rates and benthic fluxes. Quantifying the spatial–temporal dynamics in redox conditions is critical for understanding early diagenesis and argues for the use of 2D optical sensors that allow high resolution measurements of chemical species, such as pH (Hulth *et al.*, 2002; Zhu *et al.*, 2006, Larsen *et al.*, 2012), ammonia (Strömberg and Hulth, 2005) carbon dioxide (Zhu *et al.*, 2006; Schröder *et al*., 2007), ferrous iron (Zhu and Aller, 2012) and other porewater trace metals (Stahl *et al.*, 2012). The combination of measurements and transport-reaction models on appropriate spatial-temporal scales that account for the intermittency of infaunal activity are needed to better understand biogeochemical processes in biologically active sediments.

Acknowledgments and author contributions

This publication was supported by the National Science Foundation (OCE 0928002 to SAW and DSW, and OCE 0751882 to CM), the Office of Naval Research (N00014–0310352 to SAW and DSW), National Oceanic and Atmospheric Administration (NA04NOS4780264 to DSW and SAW), National Aeronautics and Space Administration (NNX11AP77 to DSW and SAW) and the Max Planck Society (LP). The Friday Harbor Laboratories of the University of Washington and Wadden Sea Station Sylt of the Alfred Wegener Institute for Polar and Marine Research in the Helmholtz Association provided laboratory and living space as well as access to field sites. Writing of the manuscript was led by NV, CM and LP, and all authors contributed intellectually to this project, which originated with NV, DSW and SAW. Data collection was done by NV, SAW and DSW; data analysis was led by NV; transport-reaction modeling was led by CM, NV and LP; optode data capture and optode and pressure data analysis software were written by LP and DSW; CP, JEH and SFT in New Zealand and AN, JN and CP in Finland (supported by the

EU BONUS+ project HYPER to AN) hosted and supported the laboratory work and specimen collection in the field. We thank Robert C. Aller and two anonymous reviewers for valuable comments on this manuscript.

Appendix

Videos 1-3: Time-lapse movies of the tellinid bivalves *Macomona liliana*, *Macoma nasuta* and *Macoma balthica* (72 hour real-time in 27 s; 9600-fold speed). Particle reworking is related to deposit-feeding activity. Occasionally the approximate position of the subsurface excurrent siphon can be deduced from the locations of ongoing particle displacement.

Video 4: Oxygen dynamics (450-fold speed) induced by intermittent irrigation by the tellinid bivalves *Macomona liliana*, *Macoma nasuta* and *Macoma balthica,* as revealed by planar optode imaging of oxygen.

References

Aller, R. C. 1980. Quantifying solute distributions in the bioturbated zone of marine sediments by defining an average microenvironment. Geochim. Cosmochim. Acta, *44*, 1955–1965.

Aller, R. C. 1994. Bioturbation and remineralization of sedimentary organic matter: effects of redox oscillation. Chem. Geol., *114*, 331–345.

Aller, R. C. and J. Y. Yingst. 1985. Effects of the marine deposit–feeders *Heteromastus filiformis* (Polychaeta), *Macoma balthica* (Bivalvia) and *Tellina texana* (Bivalvia) on averaged sedimentary solute transport, reaction rates, and microbial distributions. J. Mar. Res., *43*, 615–645.

Aller, R. C. and J. Y. Yingst. 1978. Biogeochemistry of tube-dwellings: A study of the sedentary polychaete *Amphitrite ornata* (Leidy). J. Mar. Res., *36*, 201–254.

Aller, R. C., J. Y. Yingst and W. J. Ullman. 1983. Comparative biogeochemistry of water in intertidal *Onuphis* (Polychaeta) and *Upogebia* (Crustacea) burrows: temporal pattern and causes. J. Mar. Res., *41*, 571–704.

Berg, P., S. Rysgaard, P. Funch and M. K. Sejr. 2001. Effects of bioturbation on solutes and solids in marine sediments. Aquat. Microb. Ecol., *26*, 81–94.

Bennett, W. W., P. R. Teasdale, J. G. Panther, D. T. Welsh, H. Zhao, D. F. Jolley. 2012. Investigating arsenic speciation and mobilization in sediments with DGT and DET: a mesocosm evaluation of oxic–anoxic transitions. Environ. Sci. Technol., *46*, 3981–3989.

Billerbeck, M., U. Werner, L. Polerecky, E. Walpersdorf, D. de Beer and M. Huettel. 2006. Surficial and deep pore water circulation governs spatial and temporal scales of nutrient recycling in intertidal sand flat sediment. Mar. Ecol. Prog. Ser., *326*, 61–76.

Boudreau, B. P. 2001. Solute transport above the sediment–water interface, *in* The Benthic Boundary Layer, Boudreau, B .P. and B. B. Jørgensen, eds., Oxford University Press, New York, 104–126.

Boudreau, B. P. and R. L. Marinelli. 1994. A modeling study of discontinuous biological irrigation. J. Mar. Res., *52*, 947–968.

Caradec, S., V. Grossi, F. Gilbert, C. Guigue and M. Goutx. 2004. Influence of various redox conditions on the degradation of microalgal triacylglycerols and fatty acids in marine sediments. Org. Geochem., *35*, 277–287.

Cravo–Laureau, C., G. Hernadez–Raquet , I. Vitte, R. Jézéquel, V. Bellet, J. J. Godon, P. Caumette, P. Balaguer and R. Duran. 2011. Role of environmental fluctuations and microbial diversity in degradation of hydrocarbons in contaminated sludge. Res. Microbiol., *162*, 888–895.

Dales, R. P., C. P. Mangum and J. C. Tichy. 1970. Effects of changes in oxygen and carbon dioxide concentrations on ventilation rhythms in onuphid polychaetes. J. Mar. Biol. Ass. U.K, *50*, 365–380.

D'Andrea, A. F. and T. H. DeWitt. 2009. Geochemical ecosystem engineering by the mud shrimp *Upogebia pugettensis* (Crustacea: Thalassinidae) in Yaquina Bay, Oregon: density–dependent effects on organic matter remineralization and nutrient cycling. Limnol. Oceanogr., *54*, 1911–1932.

Drent, J., P. C. Luttikhuizen and T. Piersma. 2004. Morphological dynamics in the foraging apparatus of a deposit feeding marine bivalve: phenotypic plasticity. Funct. Ecol., *18*, 349–356.

Engel, M., A. Behnke, J. Klier, C. Buschbaum, N. Volkenborn and T. Stoeck. 2012. Effects of the bioturbating lugworm *Arenicola marina* on the structure of benthic protistan communities. Mar. Ecol. Prog. Ser., *471*, 87-99.

Forster, S. and G. Graf. 1995. Impact of irrigation on oxygen flux into the sediment: intermittent pumping by *Callianassa subterranea* and "piston–pumping" by *Lanice conchilega*. Mar. Biol., *123*, 335–346.

Foster–Smith, R. L. 1978. An analysis of water flow in tube–living animals. J. Exp. Mar. Biol. Ecol., *34*, 73–95.

Gallucci, V. F. and J. Hylleberg. 1976. A quantification of some aspects of growth in the bottom–feeding bivalve *Macoma nasuta*. Veliger, *19*, 59–67.

Glud, R. N. 2008. Oxygen dynamics in marine sediments. Mar. Biol. Res., *4*, 243–289.

Glud, R. N., J. K. Gundersen, H. Røy and B. B. Jørgensen. 2003. Seasonal dynamics of benthic O_2 uptake in a semi–enclosed bay: importance of diffusion and fauna activity. Limnol. Oceanogr., *48*, 1265–1276.

Henriksen, K., M. B. Rasmussen and A. Jensen. 1983. Effect of bioturbation on microbial nitrogen transformations in the sediment and fluxes of ammonium and nitrate to the overlying water. Ecol. Bull., *35*, 193–205.

Hulth, S., R. C. Aller, P. Engstrom, and E. Selander. 2002. A pH plate fluorosensor (optode) for early diagenetic studies of marine sediments. Limnol. Oceanogr., *47*, 212–220.

Hummel, H. 1985. Food intake of *Macoma balthica* (Mollusca) in relation to seasonal changes in its potential food on a tidal flat in the Dutch Wadden Sea. Neth. J. Sea Res., *19*, 52–76

Kamermans, P. and H. J. Huitema. 1994. Shrimp (*Crangon crangon* L.) browsing upon siphon tips inhibits feeding and growth in the bivalve *Macoma balthica* (L.). J. Exp. Mar. Biol. Ecol., *175*, 59–75.

Karlson, K., E. Bonsdorff and R. Rosenberg. 2007. The impact of benthic macrofauna for nutrient fluxes from Baltic Sea sediments. Ambio, *36*, 161–167.

Klute, A. and C. Dirksen. 1986. Hydraulic conductivity and diffusivity: laboratory methods, *in* Methods of Soil Analysis, Part 1, Physical and Mineralogical Methods, A. Klute, ed., American Society of Agronomy, Madison, WI, 687–700.

Kolar, C. S. and F. J. Rahel. 1993. Interaction of a biotic factor (predator presence) and an abiotic factor (low oxygen) as an influence on benthic invertebrate communities. Oecologia, *95*, 210–219.

Kristensen, E. 1988. Benthic fauna and biogeochemical processes in marine sediments: microbial activities and flux, *in* Nitrogen Cycling in Coastal Marine Environments, Blackburn, T.H. and J. Sørensen, eds., Wiley, New York, 275–299.

Kristensen, E. 2001. Impact of polychaetes (*Nereis* spp. and *Arenicola marina*) on carbon biogeochemistry in coastal marine sediments. Geochem. Trans., *2*, 92–103.

Kristensen E., M. H. Jensen and R. C. Aller. 1991. Direct measurement of dissolved inorganic nitrogen exchange anddenitrification in individual polychaete (*Nereis virens*) burrows. J. Mar. Res., *49*, 355–377.

Larsen, M., S. M. Borisov, B. Grunwald, I. Klimant and R. N. Glud. 2012. A simple and inexpensive high resolution color ratiometric planar optode imaging approach: application to oxygen and pH sensing. Limnol. Oceanogr.: Methods, *9*, 348–360.

Le Bars, M. and M. Grae Worster. 2006. Interfacial conditions between a pure fluid and a porous medium: implications for binary alloy solidification. J. Fluid Mech., *550*, 149–173.

Levinton, J. S. 1991. Variable feeding behavior in three species of *Macoma* (Bivalvia: Tellinacea) as a response to water flow and sediment transport. Mar. Biol., *110*, 375–383.

Lin, J. and A. H. Hines. 1994. Effects of suspended food availability on the feeding mode and burial depth of the Baltic clam, *Macoma balthica*. Oikos, *69*, 28–36.

Lohrer, A. M., S. F. Thrush, M. M. Gibbs. 2004. Bioturbators enhance ecosystem function through complex biogeochemical interactions. Nature, *431*, 1092–1095.

Mangum, C. P. and L. E. Burnett. 1975. The extraction of oxygen by estuarine invertebrates, *in* Physiological Ecology of Estuarine Organisms, F. J. Vernberg, ed., University of South Carolina Press, Columbia, SC, 147–163.

Marinelli, R. L., C. R. Lovell, S. G. Wakeham, D. B. Ringelberg and D. C. White. 2002. Experimental investigation of the control of bacterial community composition in macrofaunal burrows. Mar. Ecol. Prog. Ser., *235*, 1–13.

Marinelli, R.L. and T. J. Williams. 2003. Evidence for density dependent effects of infauna on sediment biogeochemistry and benthic–pelagic coupling in nearshore systems. Estuar. Coast. Shelf Sci., *57*, 179–192.

Matsui, G.Y., N. Volkenborn, L. Polerecky, U. Henne, D. S. Wethey, C. R. Lovell and S. A. Woodin. 2011. Mechanical imitation of bidirectional bioadvection in aquatic sediments. Limnol. Oceanogr.: Methods, *9*, 84–96.

Meyerhöfer, E. 1985. Comparative pumping rates in suspension–feeding bivalves. Mar. Biol., *85*, 137–142.

Meyers, M. B., H. Fossing and E. N. Powell. 1987. Microdistribution of interstitial meiofauna, oxygen and sulfide gradients, and the tubes of macro–infauna. Mar. Ecol. Prog. Ser., *35*, 223–241.

Meysman F. J. R., O. S. Galaktionov, B. Gribsholt and J. J. Middelburg. 2006. Bio-irrigation in permeable sediments: An assessment of model complexity. J. Mar. Res., *64*, 589–627.

Meysman, F. J. R., E. S. Galaktionov and J. J. Middelburg. 2005. Irrigation patterns in permeable sediments induced by burrow ventilation: a case study of *Arenicola marina*. Mar. Ecol. Prog. Ser., *303*, 195–212.

Michaud, E., G. Desrosiers, R. C. Aller., F. Mermillod–Blondin, B. Sundby and G. Stora. 2009. Spatial interactions in the *Macoma balthica* community control biogeochemical fluxes at the sediment–water interface and microbial abundances. J. Mar. Res., *67*, 43–70.

Na, T., B. Gribsholt, O. S. Galaktionov, T. Lee and F. J. R. Meysman. 2008. Influence of advective bio–irrigation on carbon and nitrogen cycling in sandy sediments. J. Mar. Res., *66*, 691–722.

Olafsson, E. B. 1986. Density dependence in suspension–feeding and deposit–feeding populations of the bivalve *Macoma balthica*: A field experiment. J. Anim. Ecol., *55*, 517–526.

Pischedda, L., P. Cuny, J. L. Esteves, J. –C. Poggiale and F. Gilbert. 2012. Spatial oxygen heterogeneity in a *Hediste diversicolor* irrigated burrow. Hydrobiologia, *680*, 109–124.

Polerecky, L., U. Franke, U. Werner, B. Grunwald and D. de Beer. 2005. High spatial resolution measurement of oxygen consumption rates in permeable sediments. Limnol. Oceanogr.: Methods, *3*, 75–85.

Polerecky, L., N. Volkenborn and P. Stief. 2006. High temporal resolution oxygen imaging in bioirrigated sediments. Environ. Sci. Technol., *40*, 5763–5769.

Powell, A. W. B. 1979. New Zealand Mollusca: marine, land and freshwater shells. Auckland, Collins, 500 pp.

Reise, K. 1981. High abundance of small zoobenthos around biogenic structures in tidal sediments of the Wadden Sea. Helgol. Meeresunters., *34*, 413–425.

Riisgård, H. U. and P. S. Larsen. 2005. Water pumping and analysis of flow in burrowing zoobenthos–an overview. Aquat. Ecol., *39*, 237–258.

Roper, D. S., R. D. Pridmore and S. F. Thrush. 1992. Recruitment to the macrobenthos of *Macomona liliana* (Bivalvia: Tellinidae) in Manukau Harbour, New Zealand. N. Z. J. Mar. Freshwater Res., *26*, 385–392.

Schröder, C. R., L. Polerecky and I. Klimant. 2007. Time–resolved pH/pO_2 mapping with luminescent hybrid sensors. Anal. Chem., *79*, 60–70.

Schulz, H. D. 2000. Quantification of early diagenesis: Dissolved constituents in marine pore water, *in* Marine geochemistry, Schulz, H. D. and M. Zabel, eds., Springer, New York, 87–128.

Solan, M., B. D. Wigham, I. R. Hudson, R. Kennedy, C.H. Coulon, K. Norling, H.C. Nilsson and R. Rosenberg. 2004. In situ quantification of bioturbation using time–lapse fluorescent sediment profile imaging (f–SPI), luminophore tracers and model simulation. Mar. Ecol. Prog. Ser., *271*, 1–12.

Specht, D.T. and H. Lee II. 1989. Direct measurement technique for determining ventilation rate in the deposit feeding clam *Macoma nasuta* (Bivalvia, Tellinaceae). Mar. Biol., *101*, 211–218.

Stahl, H., K. W. Warnken, L. Sochaczewski, R. N. Glud, W. Davison and H. Zhang. 2012. A combined sensor for simultaneous high resolution 2–D imaging of oxygen and trace metals fluxes. Limnol. Oceanogr.: Methods, *10*, 389–401.

Stief, P., L. Polerecky, M. Poulsen and A. Schramm. 2010. Control of nitrous oxide emission from *Chironomus plumosus* larvae by nitrate and temperature. Limnol. Oceanogr., *55*, 872–884.

Stief, P., M. Poulsen, L. P. Nielsen, H. Brix and A. Schramm. 2009. Nitrous oxide emission by aquatic macrofauna. PNAS, *106*, 4296–4300.

Strömberg, N. and S. Hulth. 2005. Assessing an imaging ammonium sensor using time correlated pixel–by–pixel calibration. Anal. Chim. Acta., *550*, 61–68.

Sun, M. Y., R. C. Aller, C. Lee and S. G. Wakeham. 2002. Effects of oxygen and redox oscillation on degradation of cell associated lipids in surficial marine sediments. Geochim. Cosmochim. Acta, *66*, 2003–2012.

Sun, M. Y., C. Lee and R. C. Aller. 1993. Laboratory studies of oxic and anoxic degradation of chlorophyll–a in Long Island Sound sediments. Geochim. Cosmochim. Acta, *57*, 147–157.

Tallqvist, M. 2001. Burrowing behaviour of the baltic clam *Macoma balthica*: effects of sediment type, hypoxia and predator presence. Mar. Ecol. Prog. Ser., *212*, 183–191.

Timmermann, K., G. T. Banta and R. N. Glud. 2006. Linking *Arenicola marina* irrigation behavior to oxygen transport and dynamics in sandy sediment. J. Mar. Res., *64*, 915–938.

Volkenborn, N. and K. Reise. 2006. Lugworm exclusion experiment: responses by deposit feeding worms to biogenic habitat transformations. J. Exp. Mar. Biol. Ecol., *330*, 169–179.

Volkenborn, N., S. I. C. Hedtkamp, J. E. E. van Beusekom and K. Reise. 2007. Effects of bioturbation and bioirrigation by lugworms (*Arenicola marina*) on physical and chemical sediment properties and implications for intertidal habitat succession. Estuar. Coast. Shelf Sci., *74*, 331–343.

Volkenborn, N., L. Polerecky, D. S. Wethey and S. A. Woodin. 2010. Oscillatory porewater bioadvection in marine sediments induced by hydraulic activities of *Arenicola marina*. Limnol. Oceanogr., *55*, 1231–1247.

Volkenborn, N., L. Polerecky, D. S. Wethey, T. H. DeWitt and S. A. Woodin. 2012. Hydraulic activities by ghost shrimp *Neotrypaea californiensis* induce oxic–anoxic oscillations in sediments. Mar. Ecol. Prog. Ser., *455*, 141–156.

Vopel, K., D. Thistle and R. Rosenberg. 2003. Effect of the brittle star *Amphiura filiformis* (Amphiuridae, Echinodermata) on oxygen flux into the sediment. Limnol. Oceanogr., *48*, 2034–2045.

Wang, Y. and P. Van Cappellen. 1996. A multicomponent reactive transport model of early diagenesis: Application to redox cycling in coastal marine sediments. Geochim. Cosmochim. Acta, *60*, 2993-3014.

Werner, U., M. Billerbeck, L. Polerecky, U. Franke, M. Huettel, J. E. E. van Beusekom and D. de Beer. 2006. Spatial and temporal patterns of mineralization rates and oxygen distribution in a permeable intertidal sand flat (Sylt, Germany). Limnol. Oceanogr., *51*, 2549–2563.

Wethey, D. and S. A. Woodin. 2005. Infaunal hydraulics generate porewater pressure signals. Biol. Bull., *209*, 139–145.

Wethey, D. S., S. A. Woodin, N. Volkenborn and K. Reise. 2008. Porewater advection by hydraulic activities of lugworms, *Arenicola marina*: a field, laboratory and modeling study. J. Mar. Res., *66*, 255–273.

Woodin, S.A., R.L. Marinelli and S.M. Lindsay. 1998. Process–specific cues for recruitment in sedimentary environments: Geochemical signals? J. Mar. Res., *56,* 535–558.

Woodin, S. A., D. S. Wethey, J. E. Hewitt and S. F. Thrush. 2012. Small scale terrestrial clay deposits on intertidal sandflats: behavioral changes and productivity reduction. J. Exp. Mar. Biol. Ecol., *413*, 184–191.

Woodin, S. A., D. S. Wethey and N. Volkenborn. 2010. Infaunal hydraulic ecosystem engineers: cast of characters and impacts. Integr. Comp. Biol., *50*, 176–187.

Zhu, Q. and R. C. Aller. 2012. Two–dimensional dissolved ferrous iron distributions in marine sediments as revealed by a novel planar optical sensor. Mar. Chem., *136–137*, 14–23.

Zhu, Q., R. C. Aller and Y. Fan. 2006.. Two–dimensional pH distributions and dynamics in bioturbated marine sediments. Geochim. Cosmochim. Acta, *70*, 4933–4949.

Zwarts, L. and J. Wanink. 1989. Siphon size and burying depth in deposit– and suspension–feeding benthic bivalves. Mar. Biol., *100*, 227–24.

Figure legends

Figure 1: Porewater pressure dynamics associated with hydraulic activities of the tellinid bivalve *Macomona liliana* (shell length 5.0 cm, sediment permeability 4.3×10^{-12} m^2). The 22 hour sequence starts and ends with burrowing episodes. In between, this individual was deposit–feeding, characterized by intermittent pressurization and positive and negative hydraulic pulses associated with feces and pseudofeces expulsions and siphon movements. B and C are enlargements of the pressure data as indicated by the dashed boxes in A.

Figure 2: Intermittent porewater pressurization associated with deposit–feeding by *Macomona liliana* (shell length 4.9 cm, permeability 4.3×10^{-12} m^2), *Macoma nasuta* (shell length 4.9 cm, permeability 2.3×10^{-12} m^2) and *Macoma balthica* (shell length 2.3 cm, unknown permeability). Dotted lines indicate baseline hydrostatic pressure (p=0).

Figure 3: Temporal characteristics of intermittent porewater pressurization during deposit–feeding by tellinid bivalves. Shown are irrigation characteristics of individuals that belong to different species and size classes in sediment types with different sedimentary oxygen consumption rates (K_{OX} in μmol L_s^{-1} min^{-1}; 'na' not available). Durations of pressurized (T_{PUMP}) and non–pressurized intervals (T_{REST}) are displayed as box-and-whisker plots. Boxes correspond to the 25th and 75th percentiles, vertical lines span the 5th and 95th percentiles and the horizontal lines within the boxes correspond to the median durations. Maximal and minimal durations are indicated by small horizontal bars. Numbers in the middle correspond to the average frequencies of irrigation bouts per hour calculated as $60/(T_{PUMP}+T_{REST})$.

Figure 4: Dynamics of porewater oxygen concentrations and pressure recorded simultaneously during deposit–feeding by two tellinid species in sediments with volumetric oxygen consumption rates of 16 µmol L_s^{-1} min^{-1}. The left images are O_2 snapshots while the right images are the vertically orientated time–series of the horizontal profile indicated by dotted lines in the O_2 snapshots (a and b). The white lines in the O_2 profile time–series are the time–synchronous porewater pressure records. Pressure plateaus above the hydrostatic baseline pressure (horizontal dotted line) correspond to feeding bouts and result in oxygenation of subsurface sediment.

Figure 5: Representative spatial–temporal patterns of sediment oxygenation during 2–4 hours of deposit–feeding by 3 tellinid species. The images show (from top to bottom) the probability of oxygen being present over the analyzed period (P_{O2}), the average oxygen concentration over the oxic intervals (c_{O2}), the frequency of alterations from oxic to anoxic and back to oxic conditions per hour (F_{REDOX}), and the average durations of the oxic (T_{OX}) and anoxic (T_{ANOX}) periods. Sediment reactivity for *M. liliana* and *M. nasuta* was 16 µmol L_s^{-1} min^{-1}.

Figure 6: Modeled variations of the oxic sediment volumes (V_{O2}, defined as the volume of sediment with porewater O_2 concentrations >2 µM and below a sediment depth of 1 cm) with intermittent irrigation by tellinids. Simulations were run for 3 different sediment reactivities (K_{OX}) that approximately correspond to the range of sediment types that these bivalves inhabit – from permeable clean sand (K_{OX} = 4.5 µmol L_s^{-1} min^{-1}) to low permeability fine sand (K_{OX} = 40 µmol L_s^{-1} min^{-1}). Simulations are based on the means of the species–specific irrigation patterns derived from porewater pressure analysis and instantaneous pumping rates from the literature (*M. liliana*: Q = 1.6 mL min^{-1}; T_{PUMP} = 8.1 min; T_{REST} = 10 min; *M. nasuta*: Q = 1.8 mL min^{-1};

T_{PUMP} = 4.8 min; T_{REST} = 3.7 min; *M. balthica*: Q = 0.35 mL min^{-1}; T_{PUMP} = 2.3 min; T_{REST} = 1.7 min). Bars below species names depict the type of activity (white = rest; black = pumping).

Figure 7: Modeled variations of the oxic sediment volume, V_{O2}, around the injection pocket over a 40 min long period of constant irrigation followed by a resting period sufficiently long to reach anoxic conditions. A: Variation of V_{O2} for a specific instantaneous pumping rate (1.5 mL min^{-1}) at various sediment reactivities. B: Variation of V_{O2} for a specific sediment reactivity (18 μmol L_s^{-1} min^{-1}) and various instantaneous pumping rates. The time required to reach 95% of a steady state oxic volume (T_{O2max}) as well as the time required for a complete consumption of oxygen within the volume V_{O2max} (T_{O2zero}) are independent of the pumping rate and are governed by the reactivity of the sediment only.

Figure 8: Modeled relationships between the instantaneous pumping rates (Q) and the maximal oxic volumes (V_{O2max}) established with continuous water injection into sediments of different reactivities (K_{OX}). K_{OX} values are indicated at the distal end of the lines (A). The slope of the linear regression V_{O2max} versus Q, denoted as m, depends on K_{OX} and can be described by a hyperbolic function (B). Symbols correspond to values derived from model simulations, while solid lines correspond to the analytical approximations shown.

Figure 9: Spatio-temporal dynamics of oxygenated pockets induced by intermittent water injection into sediments of different reactivity. A and B show the fraction of V_{O2max} that is reached after a given duration of pumping and resting, assuming the initial conditions of V_{O2}=0 and V_{O2}=V_{O2max}, respectively. Symbols correspond to means obtained by modeling of the

1030 fraction of V_{O2max} established after certain T_{PUMP} and T_{REST} for 6 different pumping rates ranging
1031 from 0.1 mL min^{-1} to 3 mL min^{-1}; the error bars, if shown, would be the size of the symbol and
1032 values were not different as a function of pumping rate. Solid lines correspond to analytical
1033 approximations of V_{O2}/V_{O2max} (Eqs. 3 and 5). Panels C and D show the durations of pumping and
1034 resting that are necessary to reach 95 % and 1 % of V_{O2max} (T_{O2max} and T_{O2zero}), respectively.
1035 Filled symbols depict the means of T_{O2max} and T_{O2zero} derived from simulations with the same 6
1036 pumping rates (0.1 mL min^{-1} to 3 mL min^{-1}), while the solid lines correspond to the analytical
1037 approximations of T_{O2max} and T_{O2zero} (Eqs. 4 and 6). Open squares with error bars on the right
1038 side of C and D depict mean durations and standard deviations of tellinid irrigation bouts (T_{PUMP})
1039 and resting intervals (T_{REST}) measured with porewater pressure sensors for different tellinid
1040 species and sizes. Shown are the means of n individuals of large *M. liliana* (n=16), small *M.*
1041 *liliana* (n=7), large *M. nasuta* (n=5), and *M. balthica* (n=3). The horizontal dotted lines through
1042 the means of T_{PUMP} and T_{REST} and the vertical dotted lines from their intersections with the
1043 hyperbolic curves were added for orientation. All simulation results shown used $O_2^{injected}$ = 88
1044 μM.

1045 **Table 1:** Tellinids and sediment characteristics during porewater pressure measurements and
1046 derived behavioral time allocation to behaviors (deposit–feeding, burrowing, inactive) and
1047 temporal characteristics of intermittent irrigation during deposit–feeding. 'N' is number of
1048 individuals; 'k' is sediment permeability; 'K_{OX}' is sedimentary volumetric oxygen consumption
1049 rate; 'na' not available, *derived from time–lapse photography of 2 individuals.

Table 1 Volkenborn *et al*.

specimen			sediment characteristics				behavioral time allocation			irrigation patterns during deposit-feeding					
species	N	shell length	k	porosity	K_{OX}		deposit feeding	burrowing	inactive	bout frequency	T_{PUMP}		T_{REST}		bouts analyzed per ind.
		cm	10^{-12} m^2	vol %	µmol L_s^{-1} min^{-1}			% of time		h^{-1}	min		min		n
		mean			mean	sd					mean	sd	mean	sd	
M. liliana	8	4.7	4.3	0.49	16	2	86.2	6.3	7.5	3.4	7.7	2.3	10.5	1.9	179
M. liliana	8	4.7	0.24	0.56	43	11	89.5	6.7	3.7	3.3	8.9	2.7	9.5	1.8	139
M. liliana	4	2.4	0.10	0.56	43	11	95.8	0.9	3.2	5.6	4.4	1.0	6.7	1.8	99
M. nasuta	2	5.0	7.3	0.43	16	4	93.2	2.5	4.4	6.1	5.2	1.2	4.9	0.7	99
M. nasuta	3	5.0	2.3	0.51	31	6	85.8	3.2	11.0	8.0	4.6	0.8	2.9	0.2	129
M. balthica	3	2.1	na	na	na	na	*50.4	*0.5	*49.1	15.1	2.3	0.2	1.7	0.2	127

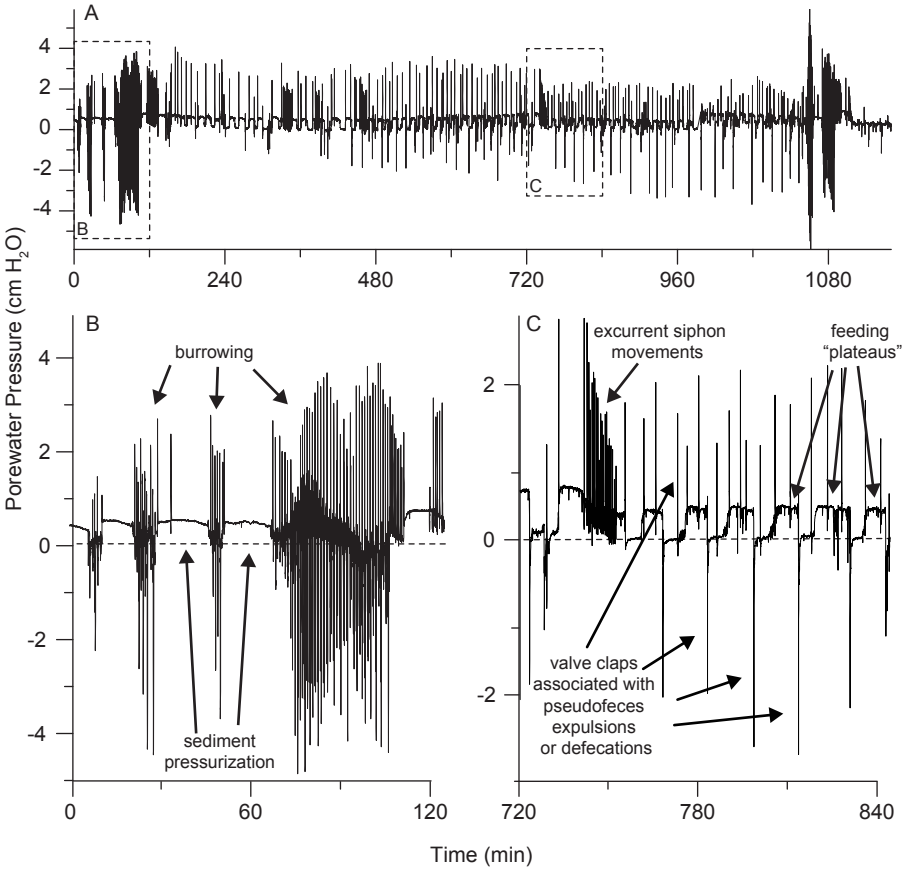

Figure 1 Volkenborn *et al.*

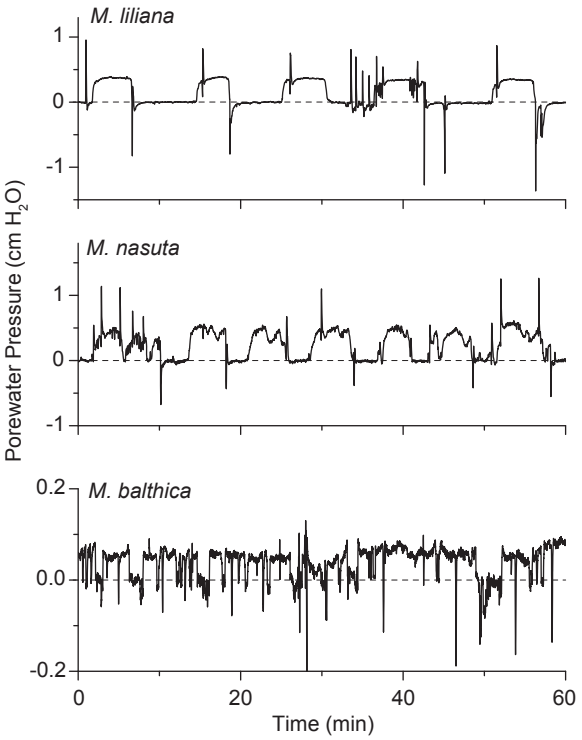

Figure 2 Volkenborn *et al.*

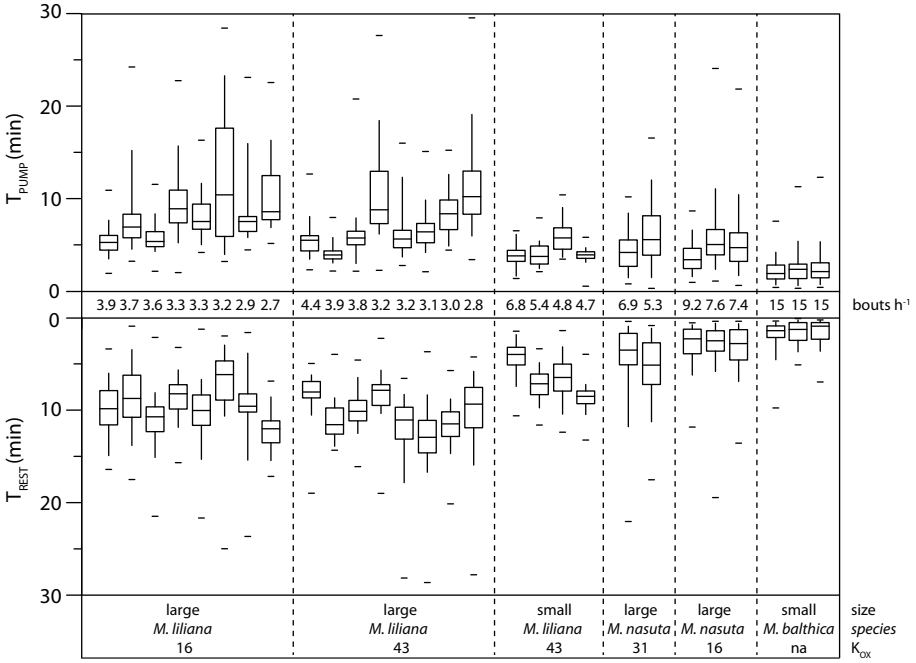

Figure 3 Volkenborn *et al.*

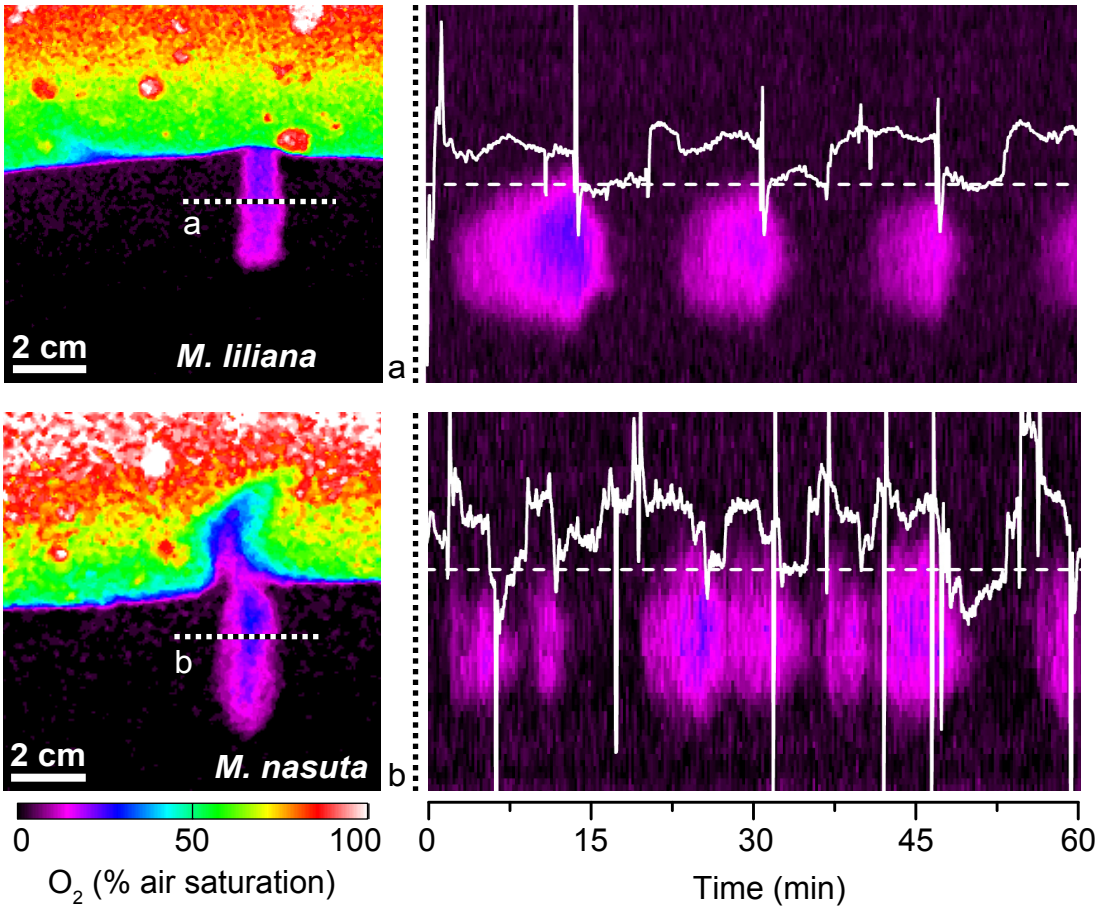

Figure 4 Volkenborn *et al.*

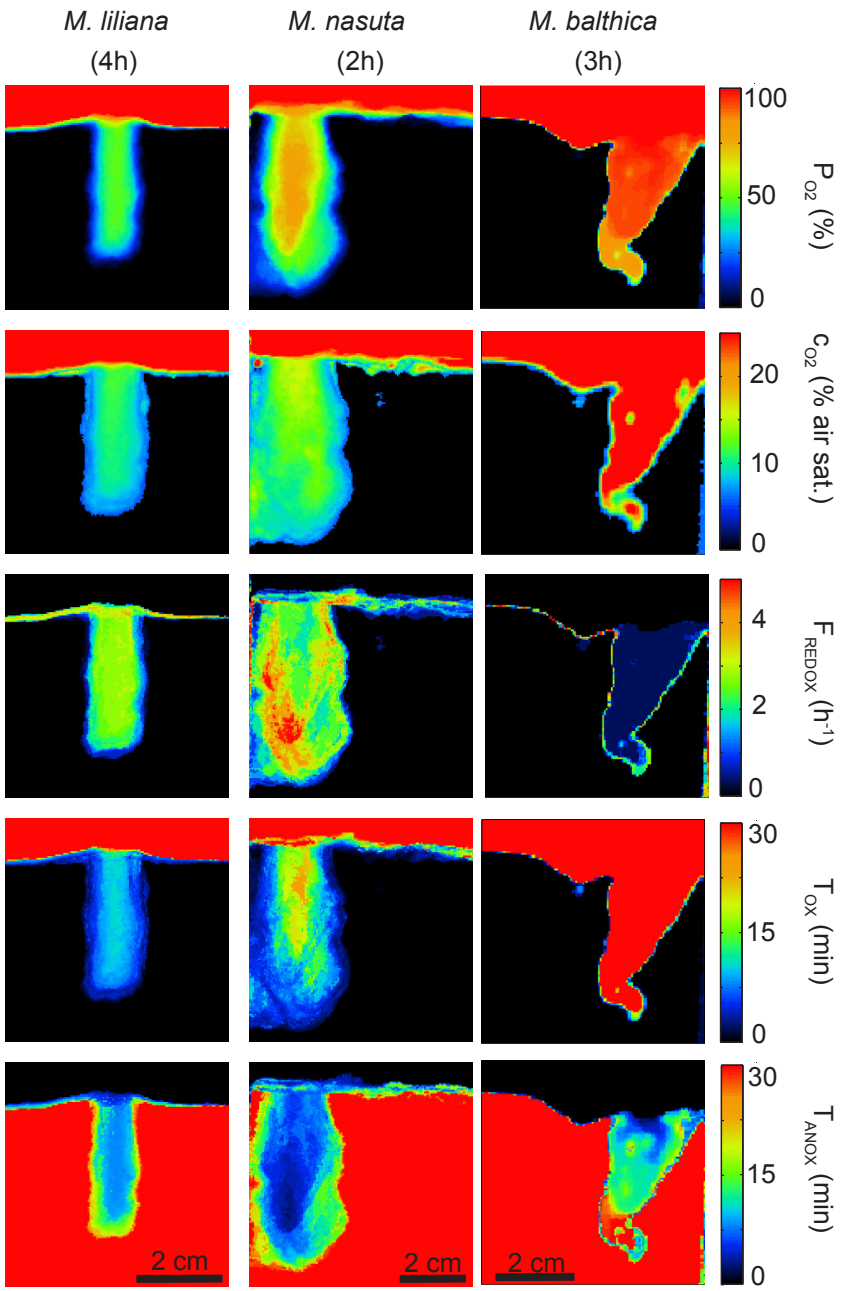

Figure 5 Volkenborn *et al.*

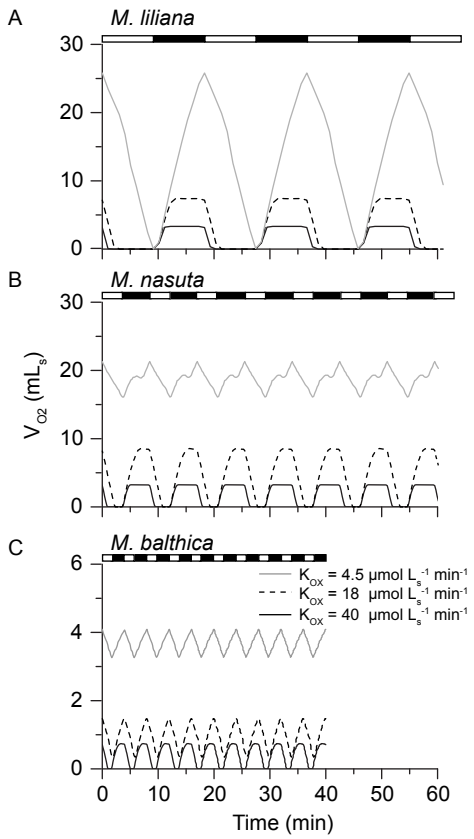

Figure 6 Volkenborn *et al.*

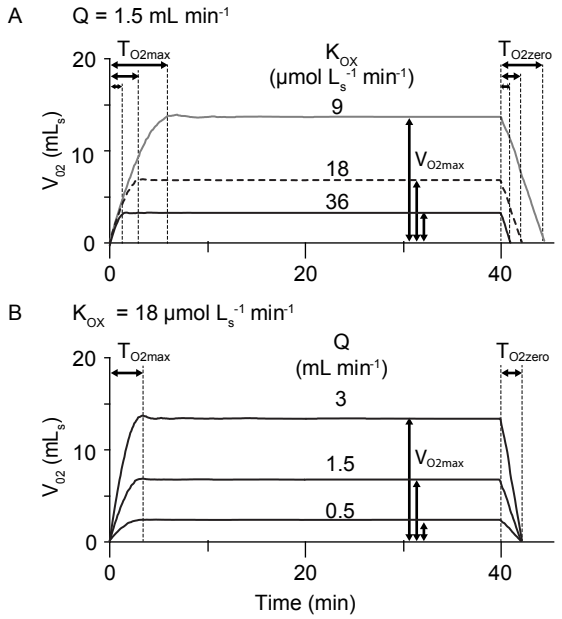

Figure 7 Volkenborn *et al*.

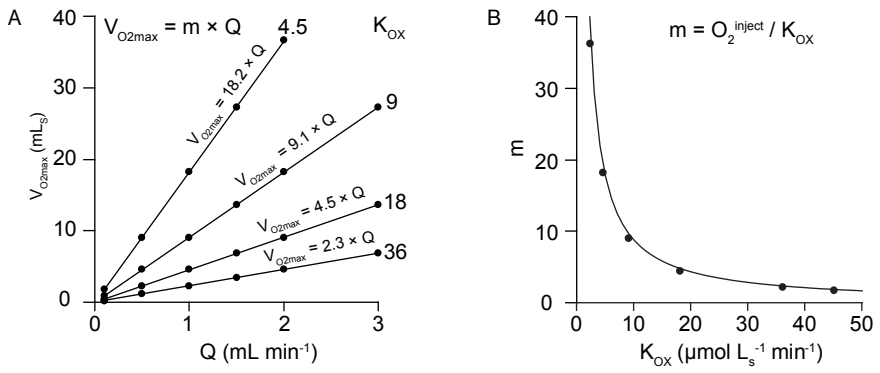

Figure 8 Volkenborn *et al*.

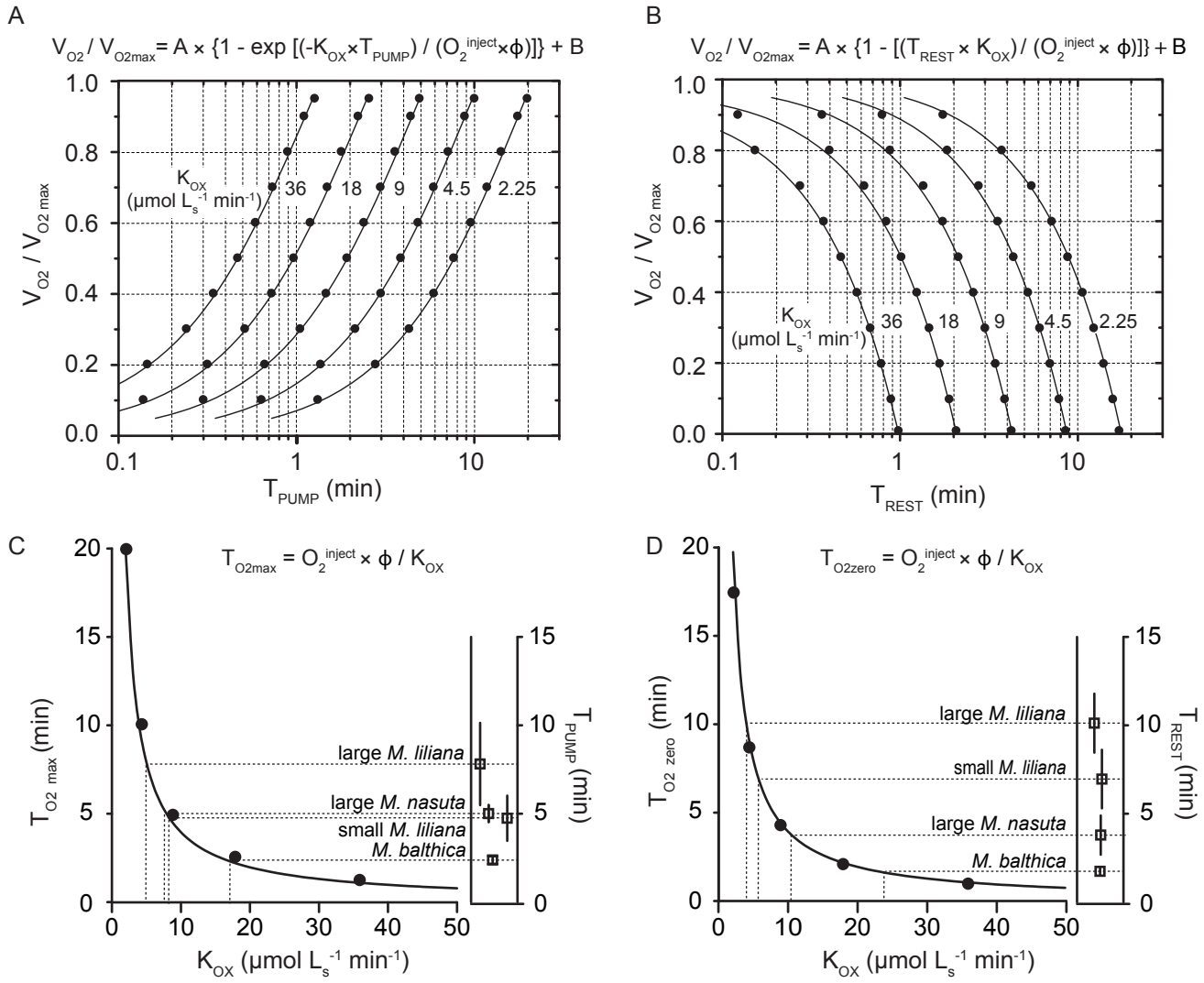

Figure 9 Volkenborn *et al.*